

New formulation of the finite depth free surface Green function

Zhimin Chen

School of Mathematics and Statistics, Shenzhen University, Shenzhen 518060, China

Abstract

For a pulsating free surface source in a three-dimensional finite depth fluid domain, there exists five images of the source due to coexistence of the free surface mirror and the water bed mirror in relation to the image method. Therefore the free surface Green function of the source is decomposed into the Rankine potential, the five image source potentials and a wave integral, of which the integrand is approximated by a smooth and rapidly decay function. The gradient Green function is further formulated so that the same integration stability with the wave integral is demonstrated. Therefore evaluation of the Green function is obtained through the integration of the integrand in a straightforward manner. This approximation is different to earlier investigations on the modifications of John's series of the Green function. The application of the scheme to a floating body or a submerged body motion in regular waves shows that the approximation is sufficiently accurate to compute linear wave loads in practice.

Keywords: Evaluation of free surface Green function; radiation waves; added mass and damping coefficients; potential flow; Hess-Smith method

1. Introduction

The understanding of wave induced forces resulting from a wave-body motion is fundamental in hydrodynamics. In the linear potential flow theory, the velocity potential of the fluid motion problem is a harmonic function and can be represented as a solution of body boundary integral equation involving free surface Green function. The integral equation can be solved numerically by combining a boundary element method for the numerical integration of the free surface Green function or free surface sources distributed on wetted body surface (see, for example, Frank [11], Lee and Sclavounos [18], Lee and Newman [20] for the infinite water depth). Thus it is fundamental for the evaluation of the free surface Green function (see, for example, the successful investigations given by Chakrabarti [2], Liang *et al.* [21], Newman [26], Noblesse [28], Ponizy *et al.* [31], Telste and Noblesse [32], Wu *et al.* [39] for the infinite depth case and John [17], Linton [23], Liu *et al.* [24], Newman [26], Pidcock [30] for the finite depth case).

For a radial symmetric body undergoing an oscillatory motion in a fluid of infinite water depth, its linear analytic solution can be approximated by a single free surface source rather than the boundary integral of free surface sources continuously distributed on the body surface. For a heaving or surging hemisphere, the velocity potential solution is decomposed into a free surface source located at the centre of the sphere and a wave-free potential, which is expanded in a series of Legendre polynomials and sinusoidal functions (see, for example, Havelock [12], Hulme

[16] and Ursell [33]). The unknown source strength and expansion coefficients are determined by the boundary condition of the velocity potential on the hemisphere. This method also applies to the wave resistance problem (see Farell [8]) of a travelling spheroid and an oscillatory submerged sphere in a fluid (see Chatjigeorgiou [3], Wang [36], Wu and Eatock Taylor [38] of infinite water depth and Linton [22] of finite water depth). Satisfactory numerical solutions can also be obtained from varieties of Rankine simple source methods on the wave body motion problem (see, for example, Cao *et al.* [1], Dawson [7], Feng *et al.* [9, 10], Mantzaris [25], Yeung [40]) by using the dynamic and kinematic free surface boundary conditions rather than the Green function theory.

In the study of the pulsating free surface Green function, the author [6] showed the singular wave integral of the Green function being approximated by a regular wave integral and the integration can be evaluated directly by using Bessel functions. The present study is a continuation of [6] to an oscillatory motion in a fluid of finite water depth.

Consider a pulsating free surface source $\mathbf{p} = (\xi, \eta, \zeta)$, in a finite depth fluid domain $-h < z < 0$, undergoing an oscillatory motion of a frequency ω . The velocity potential of the linear wave motion in the frequency domain with respect to a field point $\mathbf{q} = (x, y, z)$ is expressed as

$$\mathcal{G} = \frac{1}{4\pi} \text{Re}(G e^{-i\omega t}), \quad i = \sqrt{-1},$$

where G is a complex function expressed as

$$G = \frac{1}{r} + \frac{1}{r_0} + G_1$$

with G_1 a harmonic function in the fluid domain and

$$r = \sqrt{(x - \xi)^2 + (y - \eta)^2 + (z - \zeta)^2} \quad \text{and} \quad r_0 = \sqrt{(x - \xi)^2 + (y - \eta)^2 + (z + \zeta + 2h)^2}.$$

The function G is known as a finite depth free surface Green function or the fundamental solution of the Laplacian equation in the fluid domain associated with the free surface boundary condition and water bed boundary condition. As the Rankine source potential $\frac{1}{r}$ is the fundamental solution of the Laplacian equation in the whole three-dimensional domain, the function G is determined by the following boundary value problem:

$$\frac{\partial^2 G_1}{\partial x^2} + \frac{\partial^2 G_1}{\partial y^2} + \frac{\partial^2 G_1}{\partial z^2} = 0, \quad -h < z < 0, \quad (1)$$

$$\left. \frac{\partial G}{\partial z} - \nu G \right|_{z=0} = 0, \quad (2)$$

$$\left. \frac{\partial G}{\partial z} \right|_{z=-h} = 0, \quad (3)$$

$$\lim_{R \rightarrow \infty} \sqrt{R} \left(\frac{\partial G}{\partial R} - i\nu G \right) = 0 \quad (4)$$

for the horizontal distance $R = |(x, y) - (\xi, \eta)|$. The Green function was obtained by John [17, Eq. (A9)] as

$$G = \frac{1}{r} + \frac{1}{r_0} + \int_L \frac{2(\nu + k) e^{-kh} \cosh k(\zeta + h) \cosh k(z + h)}{k \sinh kh - \nu \cosh kh} J_0(kR) dk \quad (5)$$

for the Bessel function of the first kind J_0 and the dimensional wave number $\nu = \omega^2/g$ with g the gravitational acceleration. The wave integral pass is illustrated in Figure 1. The harmonic

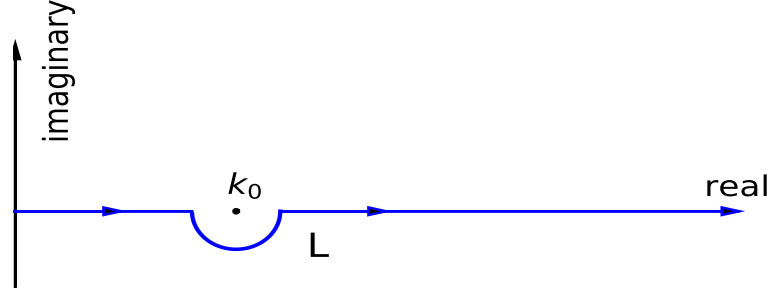


Figure 1: Profile of the integration path L in (5) passing beneath the positive root $k = k_0$.

function G_1 is an irregular wave integral due to the occurrence of the pole $k_0 > 0$, the positive root of the dispersion relation

$$k \tanh kh = \nu. \quad (6)$$

Therefore direct integration for the wave integral is not available. A well known evaluation expansion of the Green function is given by John [17, pp. 93-95] as

$$\begin{aligned} G = & 2\pi \frac{\nu^2 - k_0^2}{hk_0^2 - h\nu^2 + \nu} \cosh k_0(z + h) \cosh k_0(\zeta + h) (Y_0(k_0 R) - iJ_0(k_0 R)) \\ & + 4 \sum_{n=1}^{\infty} \frac{k_n^2 + \nu^2}{hk_n^2 + h\nu^2 - \nu} \cos k_n(z + h) \cos k_n(\zeta + h) K_0(k_n R) \end{aligned} \quad (7)$$

for Y_0 the Bessel function of the second kind and K_0 the modified Bessel function of the second kind and ik_n the roots of the dispersion relation (6) satisfying

$$\pi(n - \frac{1}{2}) \leq k_n h \leq \pi n, \quad n \geq 1.$$

For further understanding of this expansion, one may refer to Wehausen and Laitone [35, Eq. (13.19)] and Newman [26]. Eq. (7) exhibits a simple form of the Green function evaluation, which however is not a harmonic function due to the inclusion of the Rankine source singular potential $1/r$. Thus it is numerically inefficient within finite boundary elements discretisation in wave body motions. What is more, as noticed by Newman [26, p. 64], the series (7) is practically useless for small values of R/h , since each summand contains a logarithmic singularity when

$R/h = 0$. Successful developments on John's evaluation series have been obtained by many authors (see, for example, Newman [26], Liu *et al.* [24], Linton [23], Pidcock [30]).

The purpose of the present study is to approximate the three-dimensional finite depth free surface Green function through direct integration together with its application to wave body motions.

Since the integrand of the wave integral (5) has the asymptotic behaviour (as $k \rightarrow \infty$):

$$\frac{2(\nu + k)e^{-kh} \cosh k(\zeta + h) \cosh k(z + h)}{k \sinh kh - \nu \cosh kh} J_0(kR) \sim e^{k(z+\zeta)} \frac{\sqrt{2} \cos(kR + \frac{\pi}{4})}{\sqrt{\pi k R}},$$

when both the field point \mathbf{q} and the source point \mathbf{p} tend to the free surface $z = \zeta = 0$, the wave integral (5) is not stable but oscillates with unbounded amplitude. Thus it is convenient to provide a stable formulation of the Green function close to the free surface. To do so, we introduce a new formulation of the Green function expressed as

$$G = \frac{1}{r} + \frac{1}{r_0} + \frac{1}{r_1} + \frac{1}{r_2} + \frac{1}{r_3} + \frac{1}{r_4} + K \quad (8)$$

with the wave integral as the limit of smooth function integrals

$$K = \lim_{\mu \rightarrow 0+} \int_0^\infty \frac{[2\nu + (k+\nu)e^{-2kh}][e^{k(z+\zeta)} + e^{k(z-\zeta-2h)} + e^{k(-z+\zeta-2h)} + e^{-k(z+\zeta+4h)}] J_0(kR) dk}{(1+e^{-2kh})(k \tanh kh - \nu - i\mu)} \quad (9)$$

and

$$\begin{aligned} r_1 &= \sqrt{R^2 + (z + \zeta)^2}, \quad r_2 = \sqrt{R^2 + (z - \zeta + 2h)^2}, \\ r_3 &= \sqrt{R^2 + (\zeta - z + 2h)^2}, \quad r_4 = \sqrt{R^2 + (z + \zeta + 4h)^2}. \end{aligned}$$

Similar stable formulation for the gradient Green function $\nabla_{\mathbf{p}} G$ is also obtained. Thus evaluation of the Green function can be obtained by directly integrating a smooth function involving a small value of $\mu > 0$. The numerical result is accurate in comparison with that given by John's series (7). The direct integration evaluation is efficient in application to wave body motions from very good agreement of the present method results with the semi-analytic results of Wang [36], Humle[16] and Linton [23].

2. New formulation of the free surface Green function G

It is convenient to use the inverse Hankel transformation or the inverse Fourier transformation in the polar coordinate system of the horizontal plane (see, for example, [37, p. 384])

$$\frac{1}{\sqrt{R^2 + z^2}} = \int_0^\infty \frac{1}{k} e^{kz} J_0(kR) k dk = \mathcal{H}^{-1}\left(\frac{1}{k} e^{kz}\right), \quad z < 0. \quad (10)$$

It follows from (10) that, for $z + \zeta < 0$,

$$\begin{aligned} \frac{1}{r_1} + \frac{1}{r_2} + \frac{1}{r_3} + \frac{1}{r_4} &= \int_0^\infty (e^{k(z+\zeta)} + e^{k(z-\zeta-2h)} + e^{k(-z+\zeta-2h)} + e^{-k(z+\zeta+4h)}) J_0(kR) dk \\ &= \int_0^\infty 4e^{-2kh} \cosh k(\zeta + h) \cosh k(z + h) J_0(kR) dk. \end{aligned}$$

This yields that

$$\begin{aligned}
& \int_L \frac{2(\nu + k)e^{-kh} \cosh k(\zeta + h) \cosh k(z + h)}{k \sinh kh - \nu \cosh kh} J_0(kR) dk - \left(\frac{1}{r_1} + \frac{1}{r_2} + \frac{1}{r_3} + \frac{1}{r_4} \right) \\
&= \int_L \left(\frac{(\nu + k)}{(1 + e^{-2kh})(k \tanh kh - \nu)} - 1 \right) 4e^{-2kh} \cosh k(\zeta + h) \cosh k(z + h) J_0(kR) dk \\
&= \int_L \frac{[2\nu + (k + \nu)e^{-2kh}][e^{k(z+\zeta)} + e^{k(z-\zeta-2h)} + e^{k(-z+\zeta-2h)} + e^{-k(z+\zeta+4h)}]}{(1 + e^{-2kh})(k \tanh kh - \nu)} J_0(kR) dk.
\end{aligned}$$

We note that exponential functions and the Bessel function are continuous along the positive real line and thus independent of the integral pass change. Hence it remains to check the analytical behaviour of the following singular integral on the lower half circle around $k = k_0$:

$$\int_{|k-k_0|=\epsilon, \text{Im}(k)\leq 0} \frac{dk}{k \tanh kh - \nu} = \frac{1}{\tanh k_0 h} \int_{|k-k_0|=\epsilon, \text{Im}(k)\leq 0} \frac{dk}{k - k_0} = \frac{i\pi}{\tanh k_0 h} \quad (11)$$

for a given constant $\epsilon > 0$ sufficiently small. In contrast, we have integral

$$\begin{aligned}
\int_{k_0-\epsilon}^{k_0+\epsilon} \frac{dk}{k \tanh kh - \nu - i\mu} &= \frac{1}{\tanh k_0 h} \int_{k_0-\epsilon}^{k_0+\epsilon} \frac{dk}{k - k_0 - \frac{i\mu}{\tanh k_0 h}} \\
&= \frac{1}{\tanh k_0 h} \ln \frac{\epsilon \tanh k_0 h - i\mu}{-\epsilon \tanh k_0 h - i\mu} \\
&= \frac{i\pi}{\tanh k_0 h} + \frac{1}{\tanh k_0 h} \ln \left(1 + \frac{-2i\mu}{\epsilon \tanh k_0 h + i\mu} \right). \quad (12)
\end{aligned}$$

This together with (11) implies that, for any small $\epsilon > 0$,

$$\int_{|k-k_0|=\epsilon, \text{Im}(k)\leq 0} \frac{dk}{k \tanh kh - \nu} = \lim_{\mu \rightarrow 0+} \int_{k_0-\epsilon}^{k_0+\epsilon} \frac{dk}{k \tanh kh - \nu - i\mu}$$

and thus the desired formulation

$$K = \lim_{\mu \rightarrow 0+} \int_0^\infty \frac{[2\nu + (k + \nu)e^{-2kh}][e^{k(z+\zeta)} + e^{k(z-\zeta-2h)} + e^{k(-z+\zeta-2h)} + e^{-k(z+\zeta+4h)}]}{(1 + e^{-2kh})(k \tanh kh - \nu - i\mu)} J_0(kR) dk.$$

This gives the validity of (9).

The behaviour of the function $\frac{1}{k \tanh kh - \nu - i\mu}$ is displayed in Figure 2. Although this function is becoming sharper and unbounded as $\mu \rightarrow 0$, its real part is symmetric with respect to the centre point $k = k_0$, while the imaginary part tends to the dirac delta function at the vicinity of the root $k = k_0$. Thus the integral of the function around k_0 or the area bounded by the function and the real line as given by (12) is always meaningful. Therefore, the integral of the real part in the vicinity of k_0 is zero and the integral of the imaginary part around k_0 remains a constant for μ sufficiently small. However, as shown in Figure 2, the sharpness of the function increases when the parameter $\mu > 0$ decreases. Thus denser meshgrid points around k_0 are necessary for smaller $\mu > 0$.

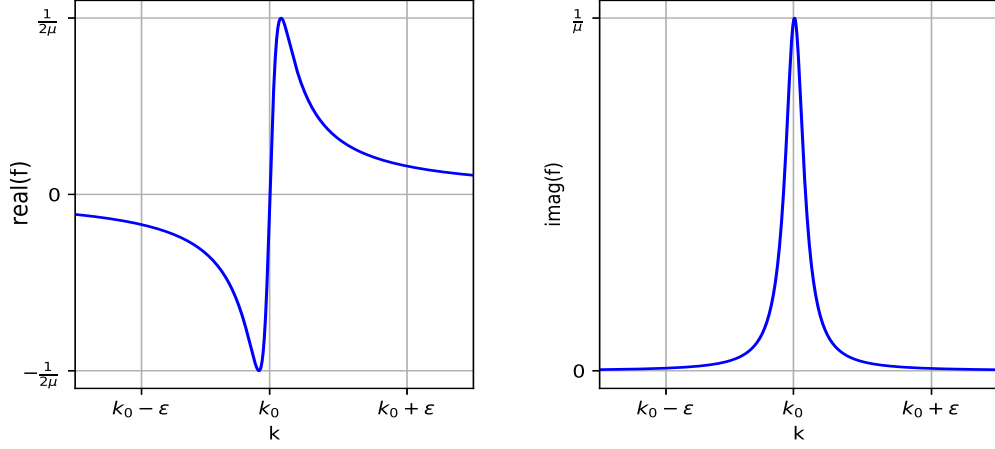


Figure 2: Profile of the smooth function $f(k) = \frac{1}{k \tanh kh - \nu - i\mu}$ around $k = k_0$.

Moreover, the dispersion relation (6) becomes the deep water dispersion relation $k - \nu = 0$ when $h\nu > 7$, since $\tanh(k_0 h) = 1$ numerically for $k_0 h > 7$. Thus compared with the infinite water depth case, the main difference of the finite water depth case is defined by the integral on the integral domain $[0, 7/\nu]$.

Next, we consider the partial derivative of K with respect to ζ . By (10), it shows that

$$\begin{aligned} \partial_\zeta K - 2\nu \left(\frac{1}{r_1} - \frac{1}{r_2} + \frac{1}{r_3} - \frac{1}{r_4} \right) \\ = \int_L \left(\frac{[2\nu + (k + \nu)e^{-2kh}]k}{(1 + e^{-2kh})(k \tanh kh - \nu)} - 2\nu \right) (e^{k(z+\zeta)} - e^{k(z-\zeta-2h)} + e^{k(\zeta-z-2h)} - e^{-k(z+\zeta+4h)}) J_0(kR) dk \\ = \int_L \frac{2\nu^2 + (k + 2\nu)(k + \nu)e^{-2kh}}{(1 + e^{-2kh})(k \tanh kh - \nu)} (e^{k(z+\zeta)} - e^{k(z-\zeta-2h)} + e^{k(\zeta-z-2h)} - e^{-k(z+\zeta+4h)}) J_0(kR) dk. \end{aligned}$$

Hence, by (13), we have

$$\begin{aligned} \partial_\zeta G - \partial_\zeta \left(\frac{1}{r} + \frac{1}{r_0} + \frac{1}{r_1} + \frac{1}{r_2} + \frac{1}{r_3} + \frac{1}{r_4} \right) - 2\nu \left(\frac{1}{r_1} - \frac{1}{r_2} + \frac{1}{r_3} - \frac{1}{r_4} \right) \\ = \lim_{\mu \rightarrow 0^+} \int_0^\infty \frac{2\nu^2 + (k + 2\nu)(k + \nu)e^{-2kh}}{(1 + e^{-2kh})(k \tanh kh - \nu - i\mu)} (e^{k(z+\zeta)} - e^{k(z-\zeta-2h)} + e^{k(\zeta-z-2h)} - e^{-k(z+\zeta+4h)}) J_0(kR) dk. \end{aligned} \quad (13)$$

Finally, for the Bessel function $J_1(s) = -\frac{dJ_0(s)}{ds}$, we have

$$\begin{aligned} \partial_R K + \int_0^\infty 2\nu (e^{k(z+\zeta)} + e^{k(z-\zeta-2h)} + e^{k(\zeta-z-2h)} + e^{-k(z+\zeta+4h)}) J_1(kR) dk \\ = - \int_L \left(\frac{[2\nu + (k + \nu)e^{-2kh}]k}{(1 + e^{-2kh})(k \tanh kh - \nu)} - 2\nu \right) (e^{k(z+\zeta)} + e^{k(z-\zeta-2h)} + e^{k(\zeta-z-2h)} + e^{-k(z+\zeta+4h)}) J_1(kR) dk \\ = - \int_L \frac{2\nu^2 + (k + 2\nu)(k + \nu)e^{-2kh}}{(1 + e^{-2kh})(k \tanh kh - \nu)} (e^{k(z+\zeta)} + e^{k(z-\zeta-2h)} + e^{k(\zeta-z-2h)} + e^{-k(z+\zeta+4h)}) J_1(kR) dk. \end{aligned} \quad (14)$$

With the use of integration by parts and (10), we have

$$\begin{aligned}
& \int_0^\infty 2\nu(e^{k(z+\zeta)} + e^{k(z-\zeta-2h)} + e^{k(\zeta-z-2h)} + e^{-k(z+\zeta+4h)})J_1(kR)dk \\
&= -\frac{2\nu}{R} \int_0^\infty (e^{k(z+\zeta)} + e^{k(z-\zeta-2h)} + e^{k(\zeta-z-2h)} + e^{-k(z+\zeta+4h)})dJ_0(kR) \\
&= \frac{8\nu}{R} + \frac{2\nu}{R} \int_0^\infty ((z+\zeta)e^{k(z+\zeta)} + (z-\zeta-2h)e^{k(z-\zeta-2h)} \\
&\quad + (\zeta-z-2h)e^{k(\zeta-z-2h)} - (z+\zeta+4h)e^{-k(z+\zeta+4h)})J_0(kR)dk \\
&= \frac{8\nu}{R} + \frac{2\nu}{R} \left(\frac{z+\zeta}{r_1} + \frac{z-\zeta-2h}{r_2} + \frac{\zeta-z-2h}{r_3} + \frac{-z-\zeta-4h}{r_4} \right) \\
&= \frac{2\nu R}{r_1(r_1+|z+\zeta|)} + \frac{2\nu R}{r_2(r_2+|z-\zeta-2h|)} + \frac{2\nu R}{r_3(r_3+|\zeta-z-2h|)} + \frac{2\nu R}{r_4(r_4+|z+\zeta+4h|)}.
\end{aligned}$$

This together with (11) and (14) implies that

$$\begin{aligned}
& \partial_R K + \frac{2\nu R}{r_1(r_1+|z+\zeta|)} + \frac{2\nu R}{r_2(r_2+|z-\zeta-2h|)} + \frac{2\nu R}{r_3(r_3+|\zeta-z-2h|)} + \frac{2\nu R}{r_4(r_4+|z+\zeta+4h|)} \\
&= -\lim_{\mu \rightarrow 0} \int_0^\infty \frac{2\nu^2 + (k+2\nu)(k+\nu)e^{-2kh}}{(1+e^{-2kh})(k \tanh kh - \nu - i\mu)} (e^{k(z+\zeta)} + e^{k(z-\zeta-2h)} + e^{k(\zeta-z-2h)} + e^{-k(z+\zeta+4h)})J_1(kR)dk.
\end{aligned}$$

This gives the formulation for the horizontal derivative of the Green function

$$\begin{aligned}
& \partial_R G - \partial_R \left(\frac{1}{r} + \frac{1}{r_0} + \frac{1}{r_1} + \frac{1}{r_2} + \frac{1}{r_3} + \frac{1}{r_4} \right) \\
&= -\lim_{\mu \rightarrow 0+} \int_0^\infty \frac{2\nu^2 + (k+2\nu)(k+\nu)e^{-2kh}}{(1+e^{-2kh})(k \tanh kh - \nu - i\mu)} (e^{k(z+\zeta)} + e^{k(z-\zeta-2h)} + e^{k(\zeta-z-2h)} + e^{-k(z+\zeta+4h)})J_1(kR)dk \\
&\quad - \left(\frac{2\nu R}{r_1(r_1+|z+\zeta|)} + \frac{2\nu R}{r_2(r_2+|z-\zeta-2h|)} + \frac{2\nu R}{r_3(r_3+|\zeta-z-2h|)} + \frac{2\nu R}{r_4(r_4+|z+\zeta+4h|)} \right). \tag{15}
\end{aligned}$$

When $h \rightarrow \infty$, the formulation reduces to the infinite depth Green function

$$G = \frac{1}{r} + \frac{1}{r_1} + \lim_{\mu \rightarrow 0+} \int_0^\infty \frac{2\nu e^{k(z+\zeta)} J_0(kR)dk}{k - \nu - i\mu} \tag{16}$$

$$\partial_\zeta G = \partial_\zeta \left(\frac{1}{r} + \frac{1}{r_1} \right) + \frac{2\nu}{r_1} + \lim_{\mu \rightarrow 0+} \int_0^\infty \frac{2\nu^2 e^{k(z+\zeta)} J_0(kR)dk}{k - \nu - i\mu} \tag{17}$$

$$\partial_R G = \partial_R \left(\frac{1}{r} + \frac{1}{r_1} \right) - \frac{2\nu R}{r_1(r_1+|z+\zeta|)} - \lim_{\mu \rightarrow 0+} \int_0^\infty \frac{2\nu^2 e^{k(z+\zeta)} J_1(kR)dk}{k - \nu - i\mu} \tag{18}$$

3. Direct integration of the Green function

Let K^μ denote the wave integral of (9) involving $\mu > 0$. By (9), (13) and (15), we have

$$K = \lim_{\mu \rightarrow 0+} K^\mu, \quad \partial_\zeta K = \lim_{\mu \rightarrow 0+} \partial_\zeta K^\mu, \quad \partial_R K = \lim_{\mu \rightarrow 0+} \partial_R K^\mu.$$

Therefore we may numerically take

$$K = K^\mu, \quad \partial_\zeta K = \partial_\zeta K^\mu, \quad \partial_R K = \partial_R K^\mu$$

for $\mu > 0$ sufficiently small.

Note that wave integral K^μ and its derivatives convergent rapidly even for the limit case $z = \zeta = 0$. The corresponding integrands are continuous throughout the integration domain $k > 0$ and decay rapidly as $k \rightarrow \infty$. The integrals can be evaluated in a straightforward manner. For simplicity, we may use the direct integration

$$\begin{aligned} K &= \sum_{j=0}^{\infty} \int_k^{k_{j+1}} \frac{[2\nu + (k + \nu)e^{-2k_j h}][e^{k(z+\zeta)} + e^{k(z-\zeta-2h)} + e^{k(-z+\zeta-2h)} + e^{-k(z+\zeta+4h)}]}{(1 + e^{-2k h})(k \tanh k h - \nu - i\mu)} J_0(kR) dk \\ &= \sum_{j=1}^{\infty} \frac{[2\nu + (k_j + \nu)e^{-2k_j h}][e^{k_j(z+\zeta)} - e^{k_j(z-\zeta-2h)} + e^{k_j(-z+\zeta-2h)} - e^{-k_j(z+\zeta+4h)}]}{(1 + e^{-2k_j h})} \\ &\quad \cdot \frac{1}{\tanh k_{j+1} h} \ln \frac{k_{j+1} \tanh k_{j+1} h - \nu - i\mu}{k_j \tanh k_{j+1} h - \nu - i\mu} J_0(k_j R). \end{aligned} \quad (19)$$

Here $\{k_j\}$ represents a set of meshgrid points of the integration domain $k > 0$.

Similarly, we have the following evaluation

$$\begin{aligned} \partial_\zeta K &= 2\nu \left(\frac{1}{r_1} - \frac{1}{r_2} + \frac{1}{r_3} - \frac{1}{r_4} \right) \\ &= \sum_{j=1}^{\infty} \int_{k_j}^{k_{j+1}} \frac{2\nu^2 + (k + 2\nu)(k + \nu)e^{-2k h}}{(1 + e^{-2k h})(k \tanh k h - \nu - i\mu)} (e^{k(z+\zeta)} - e^{k(z-\zeta-2h)} + e^{k(\zeta-z-2h)} - e^{-k(z+\zeta+4h)}) J_0(kR) dk \\ &= \sum_{j=1}^{\infty} \frac{[2\nu^2 + (k_j + 2\nu)(k_j + \nu)e^{-2k_j h}][e^{k_j(z+\zeta)} + e^{k_j(z-\zeta-2h)} + e^{k_j(-z+\zeta-2h)} + e^{-k_j(z+\zeta+4h)}]}{(1 + e^{-2k_j h})} \\ &\quad \cdot \frac{1}{\tanh k_{j+1} h} \ln \frac{k_{j+1} \tanh k_{j+1} h - \nu - i\mu}{k_j \tanh k_{j+1} h - \nu - i\mu} J_0(k_j R) \end{aligned} \quad (20)$$

and

$$\begin{aligned} \partial_R K &+ \left(\frac{2\nu R}{r_1(r_1 + |z + \zeta|)} + \frac{2\nu R}{r_2(r_2 + |z - \zeta - 2h|)} + \frac{2\nu R}{r_3(r_3 + |\zeta - z - 2h|)} + \frac{2\nu R}{r_4(r_4 + |z + \zeta + 4h|)} \right) \\ &= - \sum_{j=1}^{\infty} \frac{[2\nu^2 + (k_j + 2\nu)(k_j + \nu)e^{-2k_j h}][e^{k_j(z+\zeta)} + e^{k_j(z-\zeta-2h)} + e^{k_j(-z+\zeta-2h)} + e^{-k_j(z+\zeta+4h)}]}{(1 + e^{-2k_j h})} \\ &\quad \cdot \frac{1}{\tanh k_{j+1} h} \ln \frac{k_{j+1} \tanh k_{j+1} h - \nu - i\mu}{k_j \tanh k_{j+1} h - \nu - i\mu} J_1(k_j R) \end{aligned} \quad (21)$$

With the use of (21), we have the evaluation for the horizontal partial derivatives

$$\partial_\xi K = \partial_R K \frac{\xi - x}{R} \quad \text{and} \quad \partial_\eta K = \partial_R K \frac{\eta - y}{R}.$$

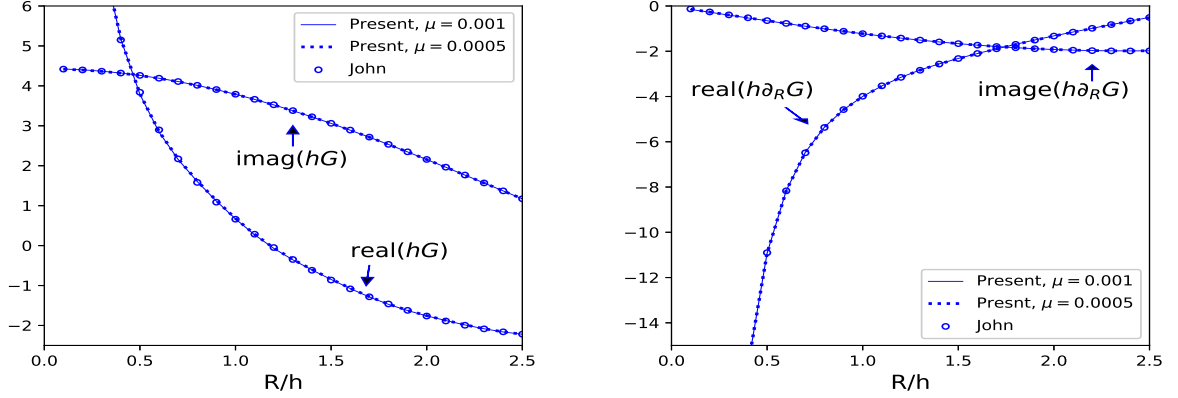


Figure 3: Influence of μ in the wave integral G and its horizontal derivative $\partial_R G$ as $\mu \rightarrow 0$ at the condition $h\nu = 0.5$.

In the numerical computation, the Green function G or the wave integral $K = K^\mu$ is now defined by the parameter $\mu > 0$. However, K^μ remains unchanged numerically for small $\mu \leq 0.01$. For displaying purpose, Figure 3 shows that G and $\partial_\zeta G$ with $\mu = 0.001$ and 0.0005 in the present evaluation are almost the same with those given by John's series (7). Thus we mainly use the value $\mu = 0.001$ in our computations.

With the use of the approximation (19)-(21), the evaluation of the Green function becomes simple but robust. To help understanding the present Green function evaluation, selected numerical results are displayed in Figure 4, which shows the accuracy of the present evaluation in comparison with John's expansion (7) for the non-dimensional wave number $h\nu$ at the moderate value $h\nu = 4$ and the small value $h\nu = 0.1$.

4. The Green function method in the wave body motion problem

Consider a three-dimensional body undergoing periodic oscillatory motion with a constant frequency ω in the fluid $-h < z < 0$, the velocity potential of the linearized oscillatory fluid motion problem can be represented as

$$\Phi = \text{Re}(\phi e^{-i\omega t}) \quad (22)$$

where the complex potential ϕ is a harmonic function satisfying the free surface boundary condition (2) and the water bed boundary condition (3). Thus ϕ is determined by the the boundary integral equation

$$\phi(\mathbf{q}) + \frac{1}{4\pi} \int_S \phi(\mathbf{p}) \frac{\partial G}{\partial \mathbf{n}_p}(\mathbf{q}, \mathbf{p}) dS_p = \frac{1}{4\pi} \int_S G(\mathbf{q}, \mathbf{p}) \frac{\partial \phi}{\partial \mathbf{n}_p}(\mathbf{p}) dS_p \quad (23)$$

for the field point \mathbf{q} in the fluid domain together with the linear body boundary condition

$$\frac{\partial \phi}{\partial \mathbf{n}_p}(\mathbf{p}) = -i\omega n_\alpha \quad \text{on } S. \quad (24)$$

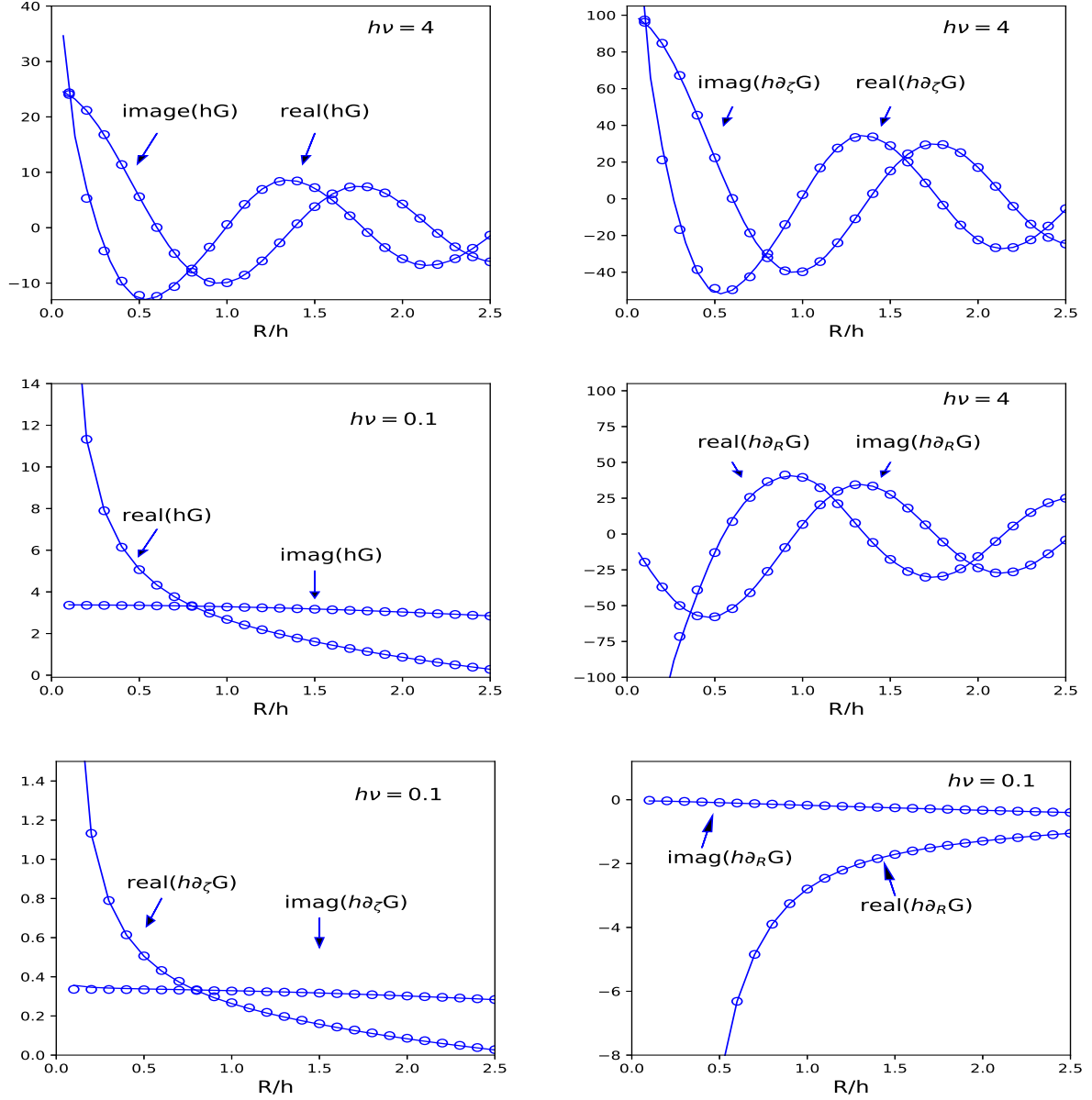


Figure 4: Comparison of the numerical Green function results given respectively by the present method (solid lines) for $\mu = 0.001$ and John's method [17] (circle lines) defined by (7).

Here S is the average wetted body surface and $\mathbf{n}_p = \mathbf{n}(\mathbf{p}) = (n_1, n_2, n_3)(\mathbf{p})$ represents the normal vector field at $\mathbf{p} \in S$ and pointing into the fluid domain. The body undergoes heave motion for $\alpha = 3$, sway motion for $\alpha = 2$ and surge motion for $\alpha = 1$.

When the field point in the fluid domain D tends to the wetted body boundary S , Eq. (23)

reduces to the boundary integral equation

$$\phi(\mathbf{q}) + \frac{1}{4\pi} \lim_{\mathbf{q}' \in D, \mathbf{q}' \rightarrow \mathbf{q}} \int_S \phi(\mathbf{p}) \frac{\partial G}{\partial \mathbf{n}_{\mathbf{p}}}(\mathbf{q}', \mathbf{p}) dS_{\mathbf{p}} = \frac{1}{4\pi} \int_S G(\mathbf{q}, \mathbf{p}) \frac{\partial \phi}{\partial \mathbf{n}_{\mathbf{p}}}(\mathbf{p}) dS_{\mathbf{p}}, \quad \mathbf{q} \in S \quad (25)$$

or the finite boundary element discretisation equation system

$$\begin{aligned} \phi(\mathbf{q}_{i,j}) + \frac{1}{4\pi} \sum_{I=1}^N \sum_{J=1}^M \phi(\mathbf{p}_{I,J}) \lim_{\mathbf{q}' \in D, \mathbf{q}' \rightarrow \mathbf{q}_{i,j}} \int_{\text{panel}_{I,J}} \frac{\partial G}{\partial \mathbf{n}_{\mathbf{p}}}(\mathbf{q}', \mathbf{p}) dS_{\mathbf{p}} \\ = \frac{1}{4\pi} \sum_{I=1}^N \sum_{J=1}^M (-i) \omega n_{\alpha}(\mathbf{q}_{I,J}) \int_{\text{panel}_{I,J}} G(\mathbf{q}_{i,j}, \mathbf{p}) dS_{\mathbf{p}}, \quad 1 \leq i \leq N, \quad 1 \leq j \leq M \end{aligned} \quad (26)$$

by using the surface mesh discretisation

$$S = \sum_{I=1}^N \sum_{J=1}^M \text{panel}_{I,J}$$

defined by mesh grid points $\mathbf{p}_{I,J}$ with $I = 1, \dots, N+1$ and $J = 1, \dots, M+1$. Here $\mathbf{q}_{I,J}$ presents the centre point of $\text{panel}_{I,J}$.

Let $|\text{panel}_{I,J}|$ denote the area of $\text{panel}_{I,J}$. The influence coefficients can be calculated as

$$\begin{aligned} \int_{\text{panel}_{I,J}} G(\mathbf{q}_{i,j}, \mathbf{p}) dS_{\mathbf{p}} \\ = \frac{1}{4\pi} \int_{\text{panel}_{I,J}} \left(\frac{1}{|\mathbf{q}_{i,j} - \mathbf{p}|} + \sum_{l=0}^4 \frac{1}{r_l(\mathbf{q}_{i,j}, \mathbf{p})} \right) dS_{\mathbf{p}} + \frac{1}{4\pi} K(\mathbf{q}_{i,j}, \mathbf{p}_{I,J}) |\text{panel}_{I,J}| \end{aligned} \quad (27)$$

and

$$\begin{aligned} \lim_{\mathbf{q}' \in D, \mathbf{q}' \rightarrow \mathbf{q}_{i,j}} \int_{\text{panel}_{I,J}} \frac{\partial G}{\partial \mathbf{n}_{\mathbf{p}}}(\mathbf{q}, \mathbf{p}) dS_{\mathbf{p}} \\ = \lim_{\mathbf{q} \in D, \mathbf{q} \rightarrow \mathbf{q}_{i,j}} \int_{\text{panel}_{I,J}} \frac{\partial \frac{1}{|\mathbf{q} - \mathbf{p}|}}{\partial \mathbf{n}_{\mathbf{p}}} dS_{\mathbf{p}} + \int_{\text{panel}_{I,J}} \sum_{l=0}^4 \frac{\partial \frac{1}{r_l(\mathbf{q}_{i,j}, \mathbf{p})}}{\partial \mathbf{n}_{\mathbf{p}}} dS_{\mathbf{p}} + \frac{\partial K(\mathbf{q}_{i,j}, \mathbf{p}_{I,J})}{\partial \mathbf{n}_{\mathbf{p}_{I,J}}} |\text{panel}_{I,J}| \end{aligned} \quad (28)$$

with

$$\lim_{\mathbf{q} \in D, \mathbf{q} \rightarrow \mathbf{q}_{i,j}} \int_{\text{panel}_{I,J}} \frac{\partial \frac{1}{|\mathbf{q} - \mathbf{p}|}}{\partial \mathbf{n}_{\mathbf{p}}} dS_{\mathbf{p}} = \int_{\text{panel}_{I,J}} \frac{\partial \frac{1}{|\mathbf{q}_{i,j} - \mathbf{p}|}}{\partial \mathbf{n}_{\mathbf{p}}} dS_{\mathbf{p}} \quad \text{when } (i, j) \neq (I, J) \quad (29)$$

$$\lim_{\mathbf{q} \in D, \mathbf{q} \rightarrow \mathbf{q}_{I,J}} \int_{\text{panel}_{I,J}} \frac{\partial \frac{1}{|\mathbf{q} - \mathbf{p}|}}{\partial \mathbf{n}_{\mathbf{p}}} dS_{\mathbf{p}} = \lim_{z \rightarrow 0^+} \int_{S_{I,J}} \frac{\partial}{\partial \hat{\zeta}} \frac{1}{\sqrt{\hat{\xi}^2 + \hat{\eta}^2 + (z - \hat{\zeta})^2}} \bigg|_{\hat{\zeta}=0} d\hat{\xi} d\hat{\eta} = 2\pi \quad (30)$$

where we have used the coordinate transformation by transform panel $_{I,J}$ in the global coordinate system on to the panel $S_{I,J}$ centered at $(0,0,0)$ in a local coordinate system $(\hat{\xi}, \hat{\eta}, \hat{\zeta})$.

The panel integrals of $\frac{1}{|\mathbf{q}_{i,j}-\mathbf{p}|}$, $\frac{1}{r_l}$ and their normal derivatives are given by the Hess-Smith quadrilateral integral method [13, 14, 27]. Therefore, with the use of the Green function approximation (19)-(21) in (27) and (28), the evaluation of the influence coefficients is obtained. Thus the algebraic equation system (26) can be numerically solved by the Gaussian elimination scheme.

5. Added mass and damping coefficients

To validate the Green function evaluation in practice and understand wave induced loading to an oscillating body in waves, we calculate numerically added mass and damping coefficients for the Green function method in wave body motions. Consider firstly a sphere of radius a submerged in the fluid $-h < z < 0$. This sphere is centred at $(0,0,-h_0)$ with $h_0/a = 1.5$ (see Figure 5)

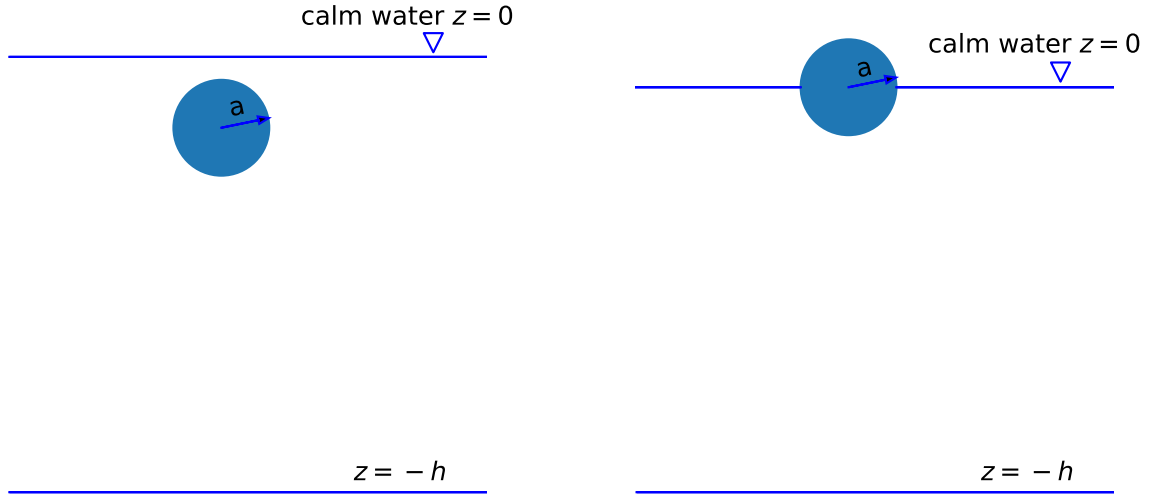


Figure 5: Cross sections ($y = 0$) of a submerged sphere of radius a centred at $(0,0,-1.5a)$ and a floating sphere of radius a .

For the numerical velocity potential solution $\phi = \phi_\alpha$ ($\alpha = 1, 2, 3$) of the boundary value problem (24) and (26), the linear hydrodynamic pressure is expressed as

$$p_\alpha = -\rho \frac{\partial \Phi_\alpha}{\partial t} = \omega \rho \text{Re} (i \phi_\alpha e^{-i\omega t})$$

for ρ the fluid density. This defines the hydrodynamic wave force exerted on the average wetted body surface S :

$$F_{\alpha,\alpha} = \int_S p_\alpha n_\alpha dS$$

and the non-dimensional added mass and damping coefficients $A_{\alpha,\alpha}$ and $B_{\alpha,\alpha}$:

$$A_{\alpha,\alpha} + iB_{\alpha,\alpha} = \frac{1}{\omega V} \int_S i\phi_\alpha n_\alpha dS = \frac{1}{\omega V} \sum_{i=1}^N \sum_{j=1}^M i\phi_\alpha(\mathbf{q}_{i,j}) n_\alpha(\mathbf{q}_{i,j}) |\text{panel}_{i,j}|. \quad (31)$$

Here V is the volume of the moving body with the wetted body surface S . Especially, $V = \frac{4}{3}\pi a^3$ for the submerged sphere and $V = \frac{2}{3}\pi a^3$ for the floating hemisphere.

Selected results of added mass and damping coefficients of heave and surge motions at different h/a values are displayed in Figure 6. For the deep water case $h/a = 10$, the present method results coincide with the semi-analytical results of Linton [22], where sway rather than surge motion is calculated. However, for the radial symmetric body, the sway motion is the same with the surge motion. Actually, for the submerged sphere oscillating at the water depth $h_0/a = 1.5$, the influence of the water bed $h/a = 10$ is negligible due to the comparison of the results with the semi-analytical results of Wang [36] in infinite water depth situation. Figure 6 also shows good agreement for the present method and Linton [22] results at $h/a = 10/3$.

Next, for the comparison with the semi-analytic results of Hulme [16] at infinite water depth, we consider a floating hemisphere (see Figure 5) undergoing respectively heave and surge motions in deep water depth. The comparison is illustrated in Figure 7. The present method results exhibit irregular frequencies at νa at the vicinity of $\nu a = 2.6$ for heaving hemisphere motion and of $\nu a = 4$ for the surging hemisphere motion. As is well known (see, Frank [11] John [17]) that the combination of panel method and free surface Green function gives rise to irregular frequencies in a high frequency range when a floating body undergoes oscillatory motions. Various methods exist (see, for example, Lee and Sclavounos [18] Ursell [34], Lee *et al.* [19] and Zhu and Lee [41]) to remove non-physical irregular frequencies. We may also use simple correction method by interpolating regular frequency data as given by the author [5] so that the smooth interpolation data for the deep water depths present excellent agreement with the results of Hulme [16]. It should be noted that the surging hemisphere oscillates in the horizontal direction and thus is not very sensitive with the water depth. Here we take $h/a = 8$ in Figure 7. Actually, the numerical results remain the same for $h/a = 4$. This case is comparable with the Smith effect. However, the heaving hemisphere oscillates in the vertical direction, we have to take much deep water depth such as $h/a = 25$ (see figure 7) to reach the infinite water depth results of Hulme [16].

6. Discussion and conclusion

To solve a wave body motion problem through a Green function method, it is necessary to evaluate the Green function G and its gradient ∇G . It is known that it is troublesome in the calculation of G and even much worse for the approximation of ∇G .

For the free surface Green function with respect to a free surface oscillating source in a fluid of infinite depth, the function G is expressed as the sum of the Rankine simple Green function $1/r$, its image $1/r_1$ with regarding to the average free water surface and a singular wave integral. Similarly, the finite depth Green function is the sum of $1/r$ and its image $1/r_0$ with respect the fluid bottom $z = -h$ and a singular wave integral G_1 (see John [17]). Under

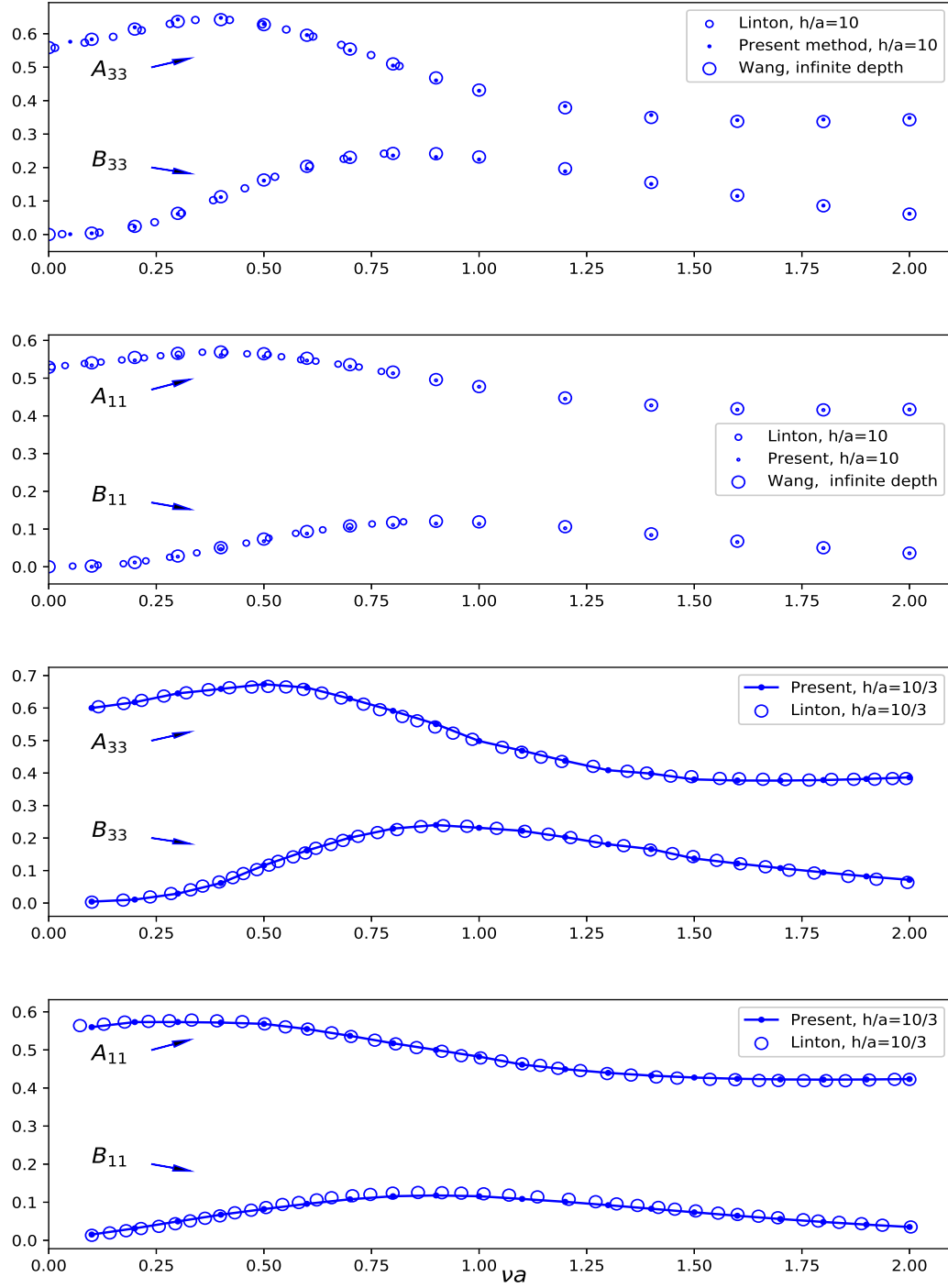


Figure 6: Added mass and damping coefficients of heaving and surging sphere of radius a submerged at the depth of $h_0 = 1.5a$ and derived by the present method and the semi-analytical methods of Wang [36] for the infinite water depth $-h \rightarrow -\infty$ and Linton [22] for finite water bed $z = -h$ values.

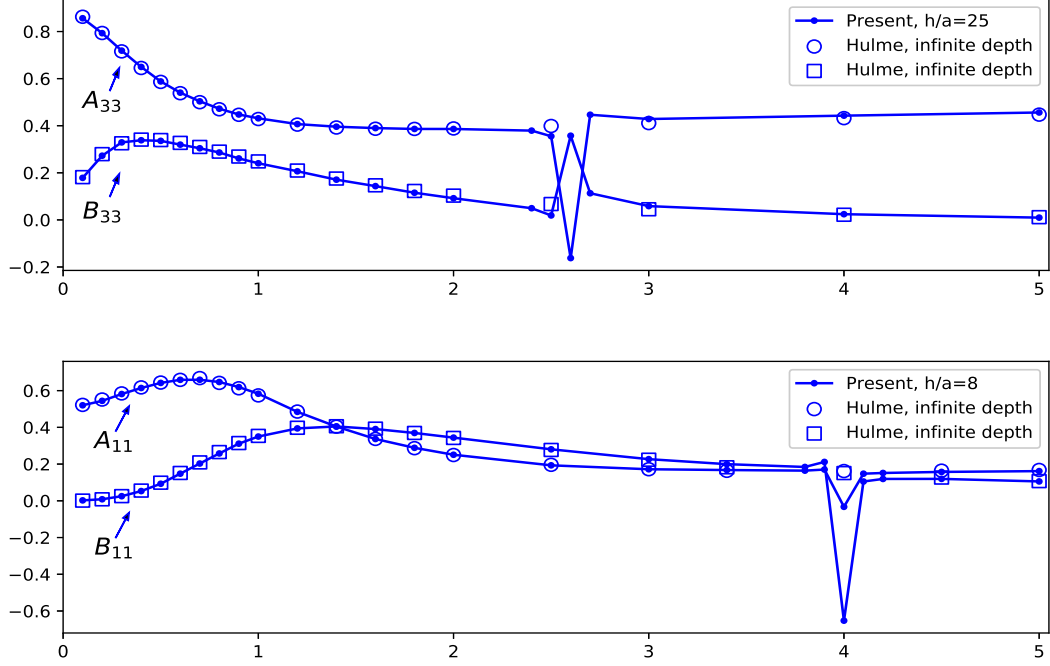


Figure 7: Added mass and damping coefficients of heaving and surging floating hemisphere of radius a derived by the present method and the semi-analytical methods of Hulme [16] for the infinite water depth $-h \rightarrow -\infty$.

this formulation, the integrand of G_1 and ∇G_1 are highly oscillating throughout the complete infinite integral domain and thus it is more difficult to be evaluated in comparison with the infinite depth Green function.

The principle difference between the infinite depth and finite depth Green functions is that the former has the single free surface mirror $z = 0$ while the latter has the additional water bed mirror $z = -h$ in relation to the image method. Due to the reflection in between the two mirrors, for a free surface source point $\mathbf{p} = (\xi, \eta, \zeta)$ in the fluid domain $-h < z < 0$, we need the following five images of \mathbf{p} :

$$\begin{aligned}
 \mathbf{p}_0 &= (\xi, \eta, -\zeta - 2h), \text{ the image of } \mathbf{p} \text{ with respect to the mirror } z = -h, \\
 \mathbf{p}_1 &= (\xi, \eta, -\zeta), \text{ the image of } \mathbf{p} \text{ with respect to the mirror } z = 0, \\
 \mathbf{p}_2 &= (\xi, \eta, \zeta - 2h), \text{ the image of } \mathbf{p}_1 \text{ with respect to the mirror } z = -h, \\
 \mathbf{p}_3 &= (\xi, \eta, \zeta + 2h), \text{ the image of } \mathbf{p}_0 \text{ with respect to the mirror } z = 0, \\
 \mathbf{p}_4 &= (\xi, \eta, -\zeta - 4h), \text{ the image of } \mathbf{p}_3 \text{ with respect to the mirror } z = -h.
 \end{aligned}$$

Therefore, in the present formulation, the Green function with respect to a field point $\mathbf{q} = (x, y, z)$ is expressed as

$$G = \frac{1}{|\mathbf{q} - \mathbf{p}|} + \sum_{n=0}^4 \frac{1}{|\mathbf{q} - \mathbf{p}_n|} + K \quad (32)$$

Here K is approximated by a wave integral, of which the integral is smooth and decay rapidly in the infinite frequency integral domain.

However, the gradient ∇K is still a highly oscillation integral. For the stability of the of the integral, ∇K is further decomposed in the a stable and regular wave integral and elementary fraction functions involving $|\mathbf{q} - \mathbf{p}_n|$.

Thus in the present formulation, the Green function is evaluated by direct integration for the wave integral. Validation of the present method is provided through comparison between the present method results and the results from John [17] series together with the added mass and damping coefficients results of Linton [22] and Wang [36] on submerged oscillatory sphere and Hulme [16] on oscillatory floating hemisphere in waves. The comparison shows that the present approximation scheme is sufficiently accurate to compute linear wave loads in practice.

This research is motivated by the direct integration approach of the wave integral [5] on double wave integral and [6] on single wave integral approximations for the three-dimensional infinite depth Green function with application to an oscillatory body motion in waves. This study is originated from [4] on two-dimensional vortex Green function method for a travelling body in fluid.

Nowadays, numerical computation of a linear hydrodynamic problem is no longer a time consuming job due to the popularization of high computing capacity computers. However, the Green function evaluation due to the presence of an irregular wave integral is known to be troublesome and sophisticated mathematical approximation theories are supposed to be employed to attack the evaluation [26, 28, 15, 29, 39]. The present investigation however shows that the singularity is removable and accurate evaluation of the Green function is obtained by an elementary integration in a straightforward manner.

Appendix A. Appendix: Green function derivation

For the completion of the analysis, we follow John [17] to show the derivation of the Green function

$$G = \frac{1}{r} + \frac{1}{r_0} + G_1.$$

The use of the Hankel transformation (10) produces

$$\mathcal{H}\left(\frac{1}{r} + \frac{1}{r_0}\right) = \frac{1}{k} \left(e^{-k|z-\zeta|} + e^{-k|z+\zeta+2h|} \right)$$

Then applying the Hankel transformation to the Laplace equation (1) and employing the bottom boundary condition (3), we have

$$\mathcal{H}(G_1) = \frac{1}{k} A_0(k) \cosh k(z+h) \quad (\text{A.1})$$

for a function A_0 . Therefore applying again the Hankel transformation to the free surface condition (2), we have, for z close to 0,

$$\begin{aligned} 0 &\approx (\partial_z - \nu) \mathcal{H}(G_1) + \partial_z \mathcal{H}\left(\frac{1}{r} + \frac{1}{r_0}\right) - \nu \mathcal{H}\left(\frac{1}{r} + \frac{1}{r_0}\right) \\ &= \frac{1}{k} A_0(k) [k \sinh k(z+h) - \nu \cosh k(z+h)] - \frac{k+\nu}{k} \left(e^{-k(z-\zeta)} + e^{-k(z+\zeta+2h)} \right) \quad (\text{A.2}) \end{aligned}$$

This implies that

$$A_0(k) = \frac{2(\nu + k)e^{-kh} \cosh k(\zeta + h)}{k \sinh kh - \nu \cosh kh}$$

Therefore the desired Green function is obtained by rewriting (A.1) as

$$G_1 = H^{-1} \left(\frac{1}{k} A_0(k) \cosh k(z + h) \right)$$

or the desired Green function

$$G = \frac{1}{r} + \frac{1}{r_0} + \int_L \frac{2(\nu + k)e^{-kh} \cosh k(\zeta + h) \cosh k(z + h)}{k \sinh kh - \nu \cosh kh} J_0(kR) dk. \quad (\text{A.3})$$

The integral pass L passing beneath the pole is determined by the asymptotic behaviour (4).

Acknowledgement. This work was partially supported by NSFC of China (11571240).

References

- [1] Y. Cao, W. Schultz, R. Beck, Three-dimensional desingularized boundary integral methods for potential problems, *Int. J. Numer. Meth. Fluids* 12 (1991) 785-803.
- [2] S.K Chakrabarti, Application and verification of deep water Green function for water waves, *J. Ship Res.* 45 (2001) 187-196.
- [3] I.K. Chatjigeorgiou, The analytic solution for hydrodynamic diffraction by submerged prolate spheroids in infinite water depth, *J. Engng. Math.* 81 (2013) 47-65.
- [4] Z.M. Chen, A vortex based panel method for potential flow simulation around a hydrofoil. *J. Fluids Struct.* 28 (2012) 378-391.
- [5] Z.M. Chen, Regular wave integral approach to numerical simulation of radiation and diffraction of surface waves, *Wave Motion* 52 (2015) 171-182.
- [6] Z.M. Chen, Straightforward integration for free surface Green function and body wave motions, *European J. Mech. / B Fluids* 74(2019) 10-18.
- [7] C.W. Dawson, A practical computer method for solving ship wave problems, In *Proceedings of 2nd International Conference on Numerical Ship Hydrodynamics*, University of California, Berkeley, 30-38, 1977.
- [8] C. Farrell, On the wave resistance of a submerged spheroid, *J. Ship Res.* 17 (1973) 1-11.
- [9] A. Feng, Z.M. Chen, W.G. Price, A Rankine source computation for three dimensional wave-body interactions adopting a nonlinear body boundary condition, *Appl. Ocean Res.* 47 (2014) 313-321.

- [10] A. Feng, Z.M. Chen, W.G. Price, A continuous desingularized source distribution method describing wave-body interactions of a large amplitude oscillatory body, *J. Offshore Mech. Arctic Engng.* 137 (2015), 021302.
- [11] W. Frank, Oscillation of cylinders in or below the free surface of deep fluids, Report 2375, Naval Ship Research Development Center, Bethesda, MD, 1967.
- [12] T. Havelock, Waves due to a floating hemi-sphere making periodic heaving oscillations, *Proc. R. Soc. Lond. A* 231 (1955) 1-7.
- [13] J.L. Hess, A.M.O. Smith, Calculation of non-lifting potential flow about arbitrary three-dimensional bodies, Report No. E.S. 40622, Douglas Aircraft Co., Inc. Aircraft Division, Long Beach, California, 1962.
- [14] J.L. Hess, A.M.O. Smith, Calculation of potential flow about arbitrary bodies, *Prog. Aerospace Sci.* 8 (1966) 1-138.
- [15] J.L. Hess and D.C. Wilcox, Progress in the solution of the problem of a three-dimensional body oscillating in the presence of a free surface - Final technical report, McDonnell Douglas Company Rep. DAC 67647, 1969.
- [16] A. Hulme, The wave forces acting on a floating hemisphere undergoing forced periodic oscillations, *J. Fluid Mech.* 121 (1982) 443-463.
- [17] F. John, On the motion of floating bodies II. Simple harmonic motions, *Communs. Pure Appl. Math.* 3 (1950) 45-101.
- [18] C.H. Lee, P.D. Sclavounos, Removing the irregular frequencies from integral equations in wave-body interactions, *J. Fluid Mech.* 207 (1989) 393-418.
- [19] C.H. Lee, J.N. Newman, X. Zhu, An extended boundary integral equation method for the removal of irregular frequency effects, *Int. J. Numer. Meth. Fluids* 23 (1996) 637-660.
- [20] C.H. Lee, J.N. Newman, Computation of wave effects using the panel method, In: S.K. Chakrabart (Ed.), *Numerical Models in Fluid-Structure Interaction*, WIT Press, Southampton, 2004.
- [21] H. Liang, H. Wu, F. Noblesse. Validation of a global approximation to the Green function of diffraction radiation in deep water, *Appl. Ocean Res.* 74 (2018) 80-86.
- [22] C. M. Linton, Radiation and diffraction of water waves by a submerged sphere in finite depth, *Ocean Engng.* 18 (1991) 61-74.
- [23] C. M. Linton, Rapidly convergent representations for Green functions for Laplace's equation. *Proc. R. Soc. A* 455 (1999) 1767-1797.
- [24] Y. Liu, H. Iwashita, C. Hu, A calculation method for finite depth free-surface green function, *Int. J. Nav. Archit. Ocean Eng.* 7 (2015) 375-389.

- [25] D.A. Mantzaris, A Rankine panel method as a tool for the hydrodynamic design of complex marine vehicles, PhD thesis, MIT, 1998.
- [26] J.N. Newman, Algorithms for the free-surface Green functions, *J. Engng. Math.* 19 (1985) 57-67.
- [27] J.N. Newman, Distributions of sources and normal dipoles over a quadrilateral panel, *J. Engng. Math.* 20 (1986) 113-126.
- [28] F. Noblesse, The Green function in the theory of radiation and diffraction of regular water waves by a body, *J. Engng. Math.* 16 (1982) 137-169.
- [29] M.A. Peter, M.H. Meylan, The eigenfunction expansion of the infinite depth free surface Green function in three dimensions, *Wave Motion* 40 (2004) 1-11.
- [30] M.K. Pidcock, The calculation of Green functions in three dimensional hydrodynamic gravity wave problems. *Int. J. Numer. Meth. Fluids* 5(1985) 891-909.
- [31] B. Ponizy, F. Noblesse, M. Ba, M. Guilbaud, Numerical evaluation of free-surface Green function, *J. Ship Res.* 38 (1994) 193-202.
- [32] J.G. Telste, F. Noblesse, Numerical evaluation of the Green function of water-wave radiation and diffraction, *J. Ship Res.* 30 (1986) 69-84.
- [33] F. Ursell, On the heaving motion of a circular cylinder on the surface of a fluid, *Quart. J. Mech Appl. Math.* 2 (1949) 218-231.
- [34] F. Ursell, Irregular frequencies and the motion of floating bodies, *J. Fluid Mech.* 105 (1981) 143-156.
- [35] J.V. Wehausen, E.V. Laitone, Surface waves, In: S. Flugge, C. Truesdell (Eds.), *Fluid Dynamics III in Handbuch der Physik* 9, Springer, Berlin, 446-778, 1960.
- [36] S. Wang, Motions of a spherical submarine in waves, *Ocean Engng.* 13 (1986) 249-271.
- [37] Watson, G. N., *A Treatise on the Theory of Bessel Functions*. Cambridge University Press, 1944.
- [38] G.X. Wu, R. Eatock Taylor, The exciting force on a submerged spheroid in regular waves, *J. Fluid Mech.* 182 (1987) 411-426.
- [39] H. Wu, C. Zhang, Y. Zhu, W. Li, D. Wan, F. Noblesse, A global approximation to the Green function for diffraction radiation of water waves, *European J. Mech. / B Fluids* 65 (2017) 54-64.
- [40] R.W. Yeung, Added mass and damping of a vertical cylinder in finite depth waters, *Appl. Ocean Res.* 3 (1981) 119-133.
- [41] X. Zhu, C.H. Lee, Removing the irregular frequencies in wave-body interactions. The 9th International Workshop on Water Waves and Floating Bodies, Japan, 245-249, 1994.